A Bayesian network approach for modeling mixed features in TCGA ovarian cancer data

Qingyang Zhang and Ji-Ping Wang, Northwestern PSOC members

***Abstract*—We propose an integrative framework to select important genetic and epigenetic features related to ovarian cancer and to quantify the causal relationships among these features using a logistic Bayesian network model based on *The Cancer Genome Atlas* data. The constructed Bayesian network has identified four gene clusters of distinct cellular functions, 13 driver genes, as well as some new biological pathways which may shed new light into the molecular mechanisms of ovarian cancer.**

I. Introduction

While the molecular mechanism of ovarian cancer remains unclear, studies have suggested that many different factors may contribute to this disease, among which there are tens of well-known oncogenes and tumor suppressors including *TP53*, *PIK3C*, *PTEN*, *BRCA1* and *BRCA2* [1,2]. However, the analysis based on individual genes often fails to provide even moderate prediction accuracy of the cancer status. Thus a systems biology approach that combines multiple genetic and epigenetic profiles for an integrative analysis provides a new direction to study the regulatory network associated with ovarian cancer. Here we describe an integrative framework that presents two innovations: (1) a novel stepwise correlation-based selector (SCBS) for important pathway-relevant features; and (2) a Bayesian network (BN) modeling for a mixture of continuous and categorical variables for casual inference. This approach provides a way to mine the massive cancer data for important genetic and epigenetic features directly or indirectly associated with cancer phenotype, leading to discoveries of pathways underlying the molecular mechanism of cancers.

II. Results

1. *Predicted Bayesian network*

We consider four important data types in our analysis in the TCGA ovarian cancer data ([1], Table 1). First, 68 potential oncogenes and tumor suppressors (identified from both literature [2] and TCGA data) were used as seed genes. An additional 271 nodes out of more than 50,000 candidate features were selected by the SCBS (Methods and [3]), including expression level of 177 genes, 82 copy number variation sites, 11 methylation sites and one somatic mutation site at gene *TP53*. The predicted BN (Fig. 1) contains many well-known biological pathways. To name a few, the edge from *CDKN2A* to *CCNE1* is a known gene-gene regulation in the RB signaling pathway [1]. The edge from *TPX2* to *AURKA* confirms that *TPX2* can activate *AURKA* by inducing autophosphorylation [4].

Table 1: Summary of TCGA ovarian cancer data

Data type	Platform	Cases
Gene expression	Agilent 244K	574 (8 organ-specific controls)
DNA methylation	Illumina 27K	584 (8 organ-specific controls)
Somatic mutation	Agilent 415K	579 (8 organ-specific controls)
Copy number	Agilent 1M	579 (8 organ-specific controls)

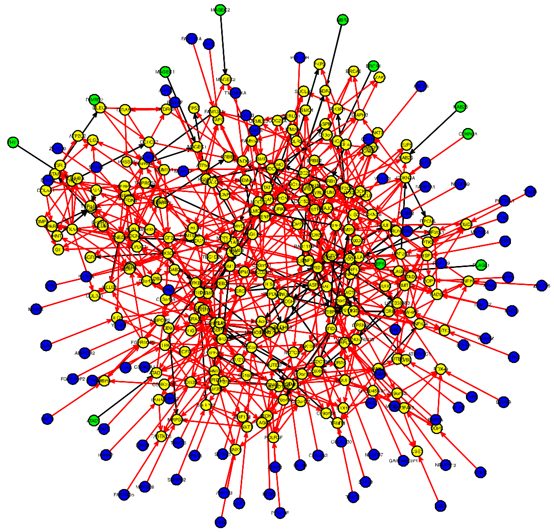

Figure 1: Predicted graph by logistic BN model with 339 nodes including expression levels of 245 genes (yellow), copy number at 82 sites (blue), methylation at 11 sites (green) and 1 somatic mutation at *TP53*. Direction of edges means the downstream feature is regulated by the upstream one. Red edges represent activation and black edges represent suppression.

2. *Hub genes and sample classification*

We identified 13 nodes with significantly larger out-degrees in the network: *ARID1A*, *C19orf53*, *CSNK2A1*, *DERL1*, *TRMT6*, *COL5A2*, *TCF21*, *LUM*, *TPX2*, *UBE2C*, DPM1, *NDUFB7* and *NDUFB9*. We show (in Fig. 2) that the 13 hub genes can clearly distinguish the cancer samples from the normal samples by a multi-dimensional scaling (MDS) plot based on the correlation dissimilarity metric (comparable clustering effect was observed based on the entire set of 245 genes). This suggests that the thirteen hub genes may present the major difference between the cancer and normal samples. The early-stage and high-grade tumor samples however are not well distinguished.

3. *Major Gene clusters*

The 245 genes fell into four major clusters corresponding to distinct functions by k-means clustering method [3]. Cluster 1 (red, Figure 3a) contained 18 genes, mainly related to cell division, mitosis, spindle formation etc. Cluster 2 (green, Figure 3a) contained 23 genes, most of which are functionally related to growth factor, cell shape, cell

Research supported by NCI grant #U54CA143869

Q. Zhang is with Department of Statistics, Northwestern University, Evanston, IL 60208, (email: QingyangZhang2015@u.northwestern.edu).

J.-P. Wang is with Department of Statistics, Northwestern University, Evanston, IL 60208, (email: jzwang@northwestern.edu)

motility, tumor invasion etc. Cluster 3 (black, Figure 3a) contained 20 genes, mostly related to mitochondrial system, membrane process etc. Cluster 4 (blue, Figure 3a) was the largest and most complicated cluster harboring 184 genes. This large cluster communicates between the other three clusters, which were nearly independent from each other (Figure 3b). These findings could be implicative of some important molecular pathways, which may or may not have been identified, that drive the development of ovarian cancer.

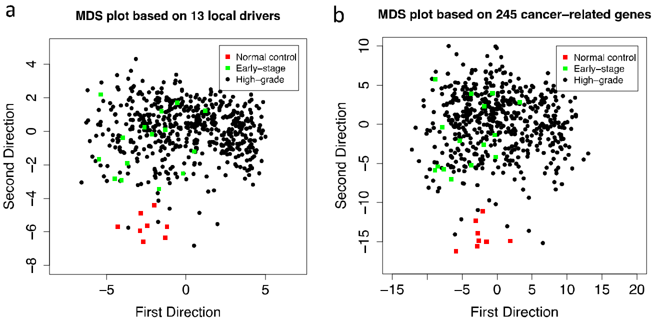

Figure 2: MDS plots for sample classification. (a) based on 13 hub genes; (b) based on all 245 genes in the predicted network. Each dot represent on sample: red (cancer-free), green (early-stage cancer) and black (high-grade cancer).

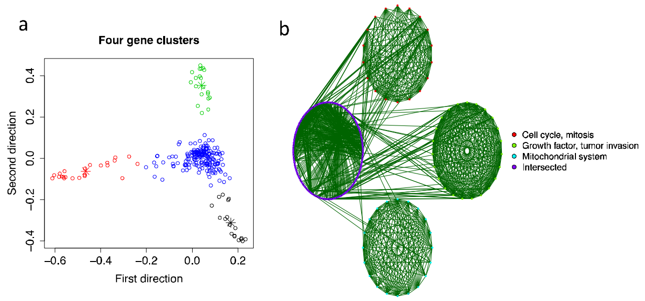

Figure 3: (a) MDS plot based on correlation dissimilarity metric between 245 genes (each circle represents one gene). Genes falling into four clusters (by k-means clustering method where k = 4) are indicated by different colors; (b) Correlation plot of the four clusters, the connection between a pair of genes represents a significant correlation.

III. Methods

1. *Bayesian network with logit link function*

The Bayesian network is one way to model the causal relationships among a set of random variables (nodes) via a directed acyclic graph ([5]). In general, the joint likelihood of nodes $X_1, X_2, \dots, X_p$ can be expressed as follows:

$$P\left(X_1, X_2, \dots, X_p\right) = \prod_{i=1}^{p} P(X_i|\Pi_i^{\mathcal{G}}), \tag{1}$$

where $\Pi_i^{\mathcal{G}}$ stands for the parental nodes of node i in the graph. The proposed logistic BN model ([3]) incorporates both continuous and discrete variables (require discretization of the continuous variables). For simplicity, we illustrate the model under binomial case:

$$\log\frac{\pi_i}{1-\pi_i} = \beta_{i0} + \sum_{j\neq i} \beta_{ij} X_j\,, \tag{2}$$

where X_i takes value 0 or 1 with respective probabilities $\{1-\pi_i, \pi_i\}$. Here we transform the network structure to the coefficient matrix $\{\beta_{ij}\}$, where $\beta_{ij} = 0$ means $X_j \nrightarrow X_i$ (no causal effect form node j to i) and otherwise $X_j \rightarrow X_i$ (with causal effect). The details of the model fitting can be found in Zhang et al [3].

2. *Stepwise correlation-based feature selector*

One important and necessary step before BN learning is feature selection. The prevailing method is based on independent test, which can falsely selects many irrelevant features as some features could be causal to other features while having no direct association with the cancer phenotypes. With the SCBS procedure, we start with detection of features significantly correlated with the cancer and then progressively select subsequent features that correlate with the selected features. Suppose we aim to select p variables (out of S candidates, $S \gg p$) as the nodes in BN based on N random samples. SCBS can be implemented as follows:

Step 1: Calculate the correlation coefficients between the current node X_i and all the other nodes. Keep k most correlated nodes with X_i for further filtering.
Step 2: Calculate the p-value of correlation coefficient for each of the k nodes from step 1, Select the node if the p-value is significant under Benjamini-Hochberg procedure with $\text{FDR} \leq 0.05$.
Step 3: Repeat step 1 and 2 until p nodes are selected.

For the choice of k, we suggest k = 4, 5 or 6 in practice since smaller k tends to miss weakly connected nodes and larger k tends to catch more false positives. See a simulation study in [3] for detail.

References

[1] The Cancer Genome Atlas Research Network, “Integrated genome analyses of ovarian carcinoma”, *Nature*, vol.474, pp. 609-615

[2] R. Bast, B. Hennessy and G. Mills, “The biology of ovarian cancer: new opportunities for translation”, *Nature Cancer Review*, vol. 9, pp. 415-428, 2009

[3] Q. Zhang, J.E. Burdette and J.-P. Wang, “Integrative network analysis of TCGA data for ovarian cancer”, *BMC Systems Biology*, vol. 8, No. 1338, pp. 1-18, 2014

[4] T. Kufer, H. Sillje, R. Korner, O. Gruss, P. Meraldi and E. Nigg, “Human TPX2 is required for targeting Aurora-A Kinase to the spindle”, *Journal of Cell Biology*, vol. 158, No. 4, pp. 617-623, 2002

[5] P. Spirtes, C. Glymour and R. Scheine, *Computation, Causation and Discovery*. Cambridge: Springer, 1993

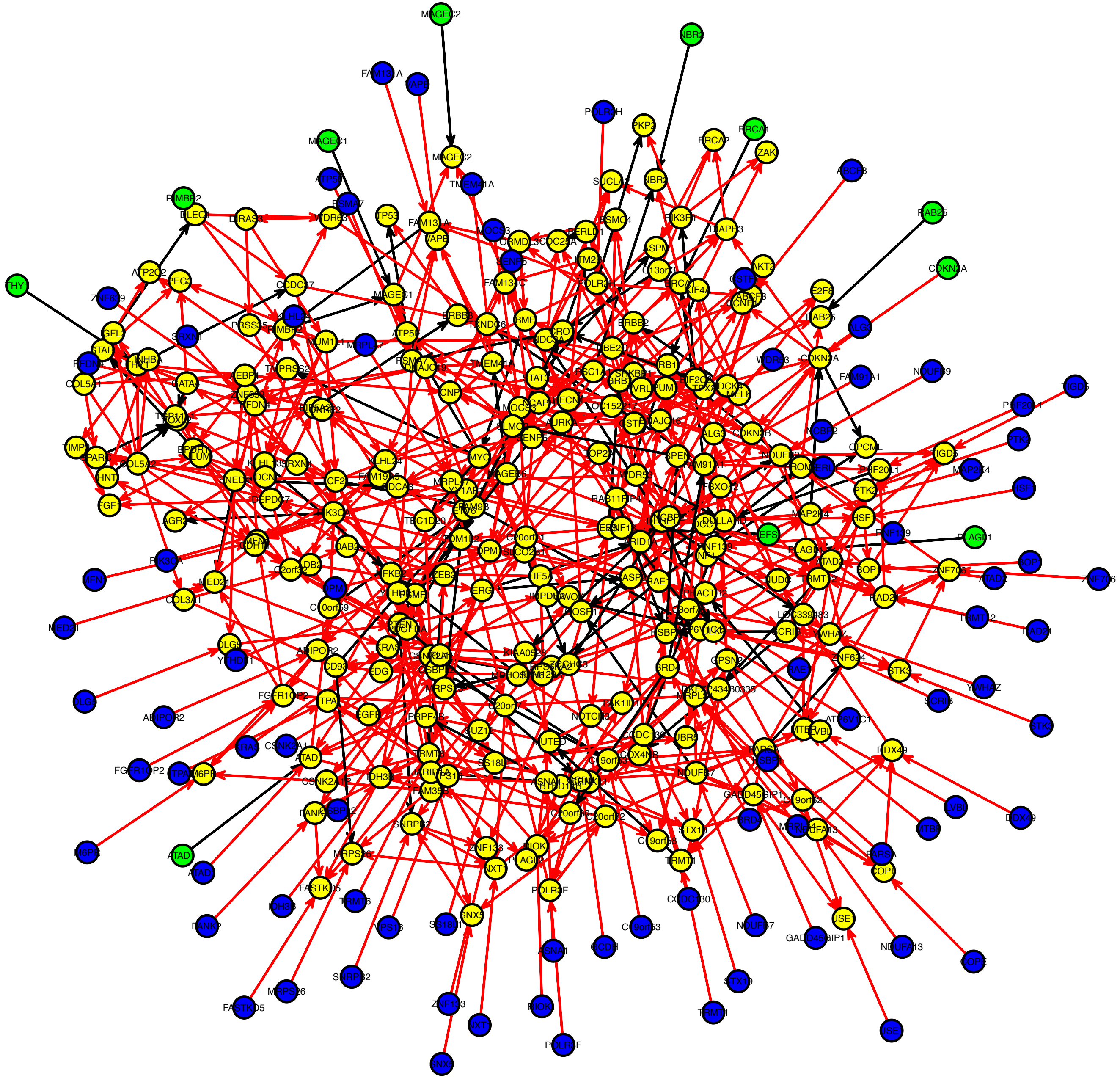
MAGEC2
NBR2
FAM131A
VAPB
POLR2H
PKP2
BRCA2
BRCA1
ZAK
MAGEC1
MAGEC2
ABCF3
ATP5E
TMEM41A
SUCLA2
NBR2
RAB25
RIMBR2
DLEC1
DIRAS3
WDR63
PSMA7
TP53
FAM131A
VAPB
PIK3R1
DIAPH3
CDKN2A
MOCS3
ORMDL3
CDC25A
PERLD1
PSMC4
ASPN
C13orf3
SENP5
ITM2B
AKT2
THY1
ATP2C2
PEG3
CCDC37
FAM134C
POLR2I
BRCA1
KIF4A
GSTP1
ABCF3
E2F8
ZNF589
MAGEC1
KLHL24
CCNE1
IGFL2
PRSS35
RIMBR2
MUM1L1
ERBB3
TKNDC6
BMF
CROT
ERBB2
RAB25
ALG3
STAP
SRXN1
MRPL17
ATP5E
INHBA
PSMA7
DNAJC19
TMEM41A
UBE2D1
WDR53
CDKN2A
FAM91A1
NDUFB9
TIGD5
RFDN4
THY1
GATA4
EEBP4
TMPRSS2
CNP
STAT3
TSC1
RB1
EIF2C2
DCK
COL5A1
ZNF639
SPIKBP1
GRB1
PUM1
TFX2
MELK
PHF20L1
RFDN4
EIF5A2
MOCS3
CAPN
LOC152217
TPBX1
FOXJ1
SLMO2
AURKA
GSTP1
DNAJC19
ALG3
CDKN2B
ICBP2
PTK2
SENP5
TOP2A
SPEN
NDUFB9
CPCML
TIMP1
SPARC
COL5A2
EPDR1
LUM
KLHL13
SRXN1
KLHL24
MYC
FAM91A1
TIGD5
MAP2K4
HNT
SNED1
DCN
CF2
FAM19A5
MRPL17
MAGEB2
WDR53
PHF20L1
HSF1
DEPDC7
CDCA8
RAB11FIP4
FBXO42
PTK2
FGF1
AGR2
PIK3CA
TBC1D20
FAM98
MAP2K4
HSF1
HSBP1
DOLLAR
EEFS
RNF139
PLAGL1
EEFS
RNF139
TDM1L2
C20orf11
ARID1A
MFN1
DAB2
DPM1
PLAGL1
ATAD2
BOP1
ZNF706
BOP1
PIK3CA
C2orf32
NFKB2
ZEB2
EIF5A
SOCO2B1
RAE1
MFN
MED21
DPM
YTHDF3
PSMF1
ERG
IMPDH2
CASP
TRMT12
NUDC
ZNF706
ATAD2
COL3A1
C10orf59
COSF1
C8orf7
PHACTR2
RAD21
LOC339483
TRMT12
MED21
PTEN
PDGFRA
HSBP1
SCRIB
YWHAZ
RAD21
DLG5
YTHDF1
KRAS
ADIPOR2
KIAA0528
CSNK2A1
ZC3H3
BRD4
GPSN2
RAE1
ZNF624
STK3
CD93
EDG1
CBSPH
MRPS1
HOS3
FAM120
DKFZP434B0335
YWHAZ
SCRIB
DLG5
FGFR1OP2
ITPA
ADIPOR2
EGFR
C20orf7
NOTCH3
PAK1IP1
MRPL3
ATP6V1C1
STK3
PRPF4B
SUZ12
MTBP
LVBL
CSNK2A1
KRAS
ATAD
CCDC130
UBR5
FARSA
DDX49
FGFR1OP2
ITPA
M6PR
TRMT6
MUTED
C19orf53
CDX4NB
HSBP1
JARID1A
SS18L1
CSNK2A1P
IDH3B
VPS16
NDUFB7
ASNA1
GCDH
CTDNK1
GADD45GIP1
C19orf52
RANK2
GADD45GIP1
SRPL2
FAM35B
C20orf30
C20orf72
BRD4
MRPL34
NDUFA13
LVBL
MTBP
DDX49
M6PR
ATAD
SNRPB2
ZNF133
RIOK1
C19orf58
STX10
MRPS26
NXT1
PLAGL2
TRMT1
FARSA
COPE
ATAD
POLR3F
CCDC130
FASTK05
IDH3B
TRMT6
SNX5
C19orf53
USE1
NDUFB7
GADD45GIP1
NDUFA13
COPE
RANK2
VPS16
SS18L1
ASNA1
GCDH
SNRPB2
STX10
FASTK05
MRPS26
ZNF133
RIOK1
TRMT1
USE1
NXT1
POLR3F
SNX5

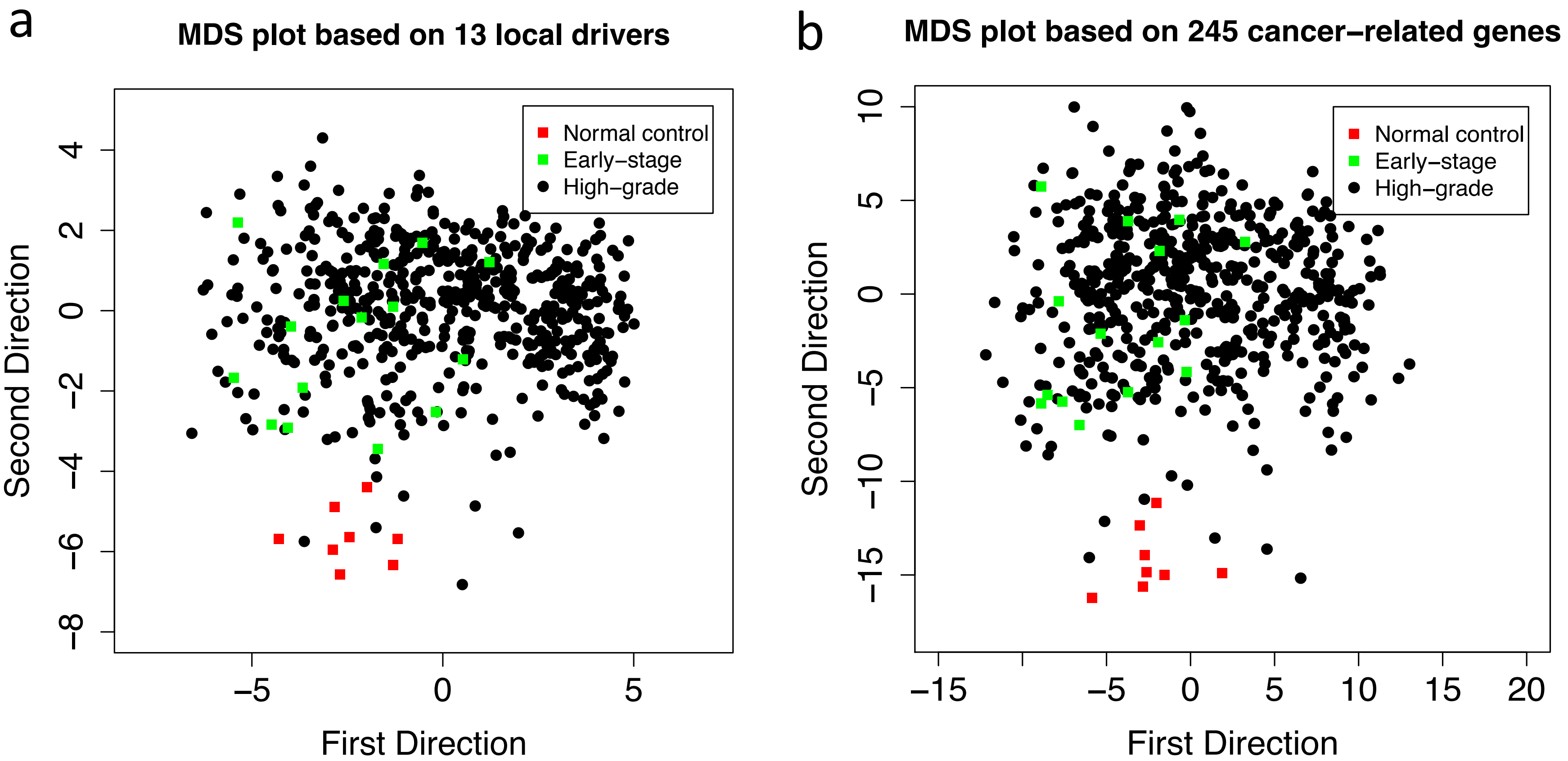
a
MDS plot based on 13 local drivers
Normal control
Early–stage
High–grade
Second Direction
4
2
0
−2
−4
−6
−8
−5
0
5
First Direction
b
MDS plot based on 245 cancer–related genes
Normal control
Early–stage
High–grade
Second Direction
10
5
0
−5
−10
−15
−15
−5
0
5
10
15
20
First Direction

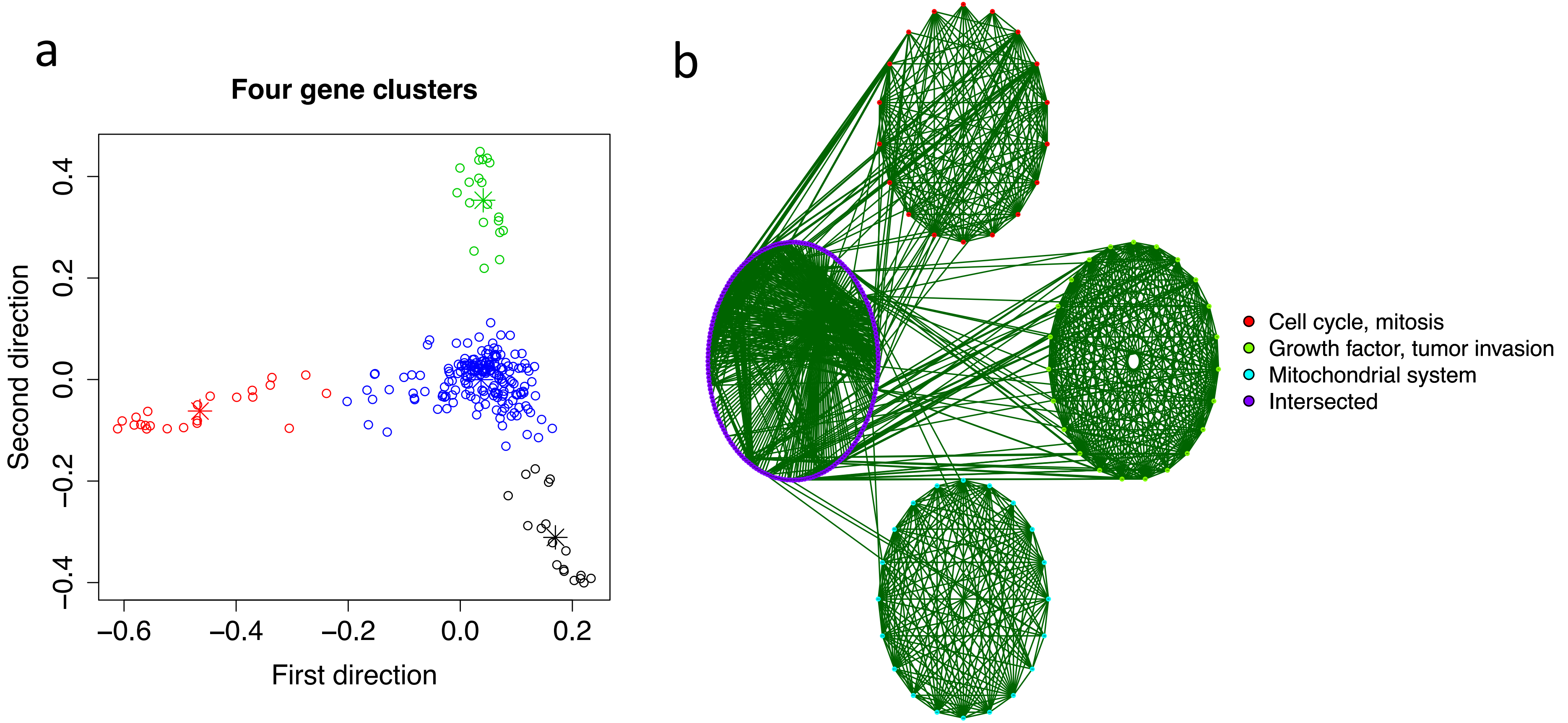
a
Four gene clusters
Second direction
First direction
0.4
0.2
0.0
−0.2
−0.4
−0.6
−0.4
−0.2
0.0
0.2
b
● Cell cycle, mitosis
● Growth factor, tumor invasion
● Mitochondrial system
● Intersected